

Using Bayesian Inference to Distinguish Neutrino Flavor Conversion Scenarios via a Prospective Supernova Neutrino Signal

Sajad Abbar ¹ and Maria Cristina Volpe²

¹*Max-Planck-Institut für Physik (Werner-Heisenberg-Institut), Boltzmannstr. 8, 85748 Garching, Germany*

²*Astro-Particule et Cosmologie (APC), CNRS UMR 7164, Université Denis Diderot, 10, rue Alice Domon et Leonie Duquet, 75205 Paris Cedex 13, France*

The upcoming galactic core-collapse supernova is expected to produce a considerable number of neutrino events within terrestrial detectors. By using Bayesian inference techniques, we address the feasibility of distinguishing among various neutrino flavor conversion scenarios in the supernova environment, using such a neutrino signal. In addition to the conventional MSW, we explore several more sophisticated flavor conversion scenarios, such as spectral swapping, fast flavor conversions, flavor equipartition caused by non-standard neutrino interactions, magnetically-induced flavor equilibration, and flavor equilibrium resulting from slow flavor conversions. Our analysis demonstrates that with a sufficiently large number of neutrino events during the supernova accretion phase (exceeding several hundreds), there exists a good probability of distinguishing among feasible neutrino flavor conversion scenarios in the supernova environment.

I. INTRODUCTION

Neutrinos originating from core-collapse supernovae (CCSNe) present an unprecedented opportunity for exploring the intricacies of astroparticle physics. Understanding the behavior and characteristics of these neutrinos can significantly contribute to the broader comprehension of neutrino physics in extreme conditions and offers invaluable insights into the physics governing the CCSNe [1–4].

Since the detection of Supernova 1987A (SN 1987A) and its corresponding neutrino signal, there has been a substantial body of research focusing on studying a galactic SN neutrino signals for various purposes. These studies have focused on a number of issues, such as developing insight into the SN explosion mechanism [5, 6], understanding neutrino spectral parameters [7–9], analyzing SN remnant features [10, 11], and exploring non-standard physics in extreme conditions [12–14]. Specifically, Refs. [15–17] have recently employed Bayesian techniques to differentiate between various SN models by analyzing a future SN neutrino signal.

One of the most captivating aspects of SN neutrinos is that they are thought to undergo a phenomenon known as *collective* neutrino oscillations [4, 18–24]. This intriguing behavior arises from an intricate interplay between propagating neutrinos and the dense background neutrino gas, where the coherent forward scatterings of neutrinos play a major role. What makes this phenomenon particularly fascinating is its nonlinear and collective nature.

The phenomenon of neutrino flavor conversion (FC) within the SN environment displays a remarkable richness. It has been established that varying the physics conditions in the SN environment can give rise to different FC scenarios. While the conventional Mikheev-Smirnov-Wolfenstein (MSW) effect arises from a resonant behavior resulting from the interplay between matter and vacuum Hamiltonian terms, the SN environment

introduces more intricate FC scenarios for neutrinos.

Initially, the understanding of neutrino FCs in the SN environment was mostly centered around the so-called phenomenon of slow modes (driven by the neutrino vacuum frequency), and specifically the well-established phenomenon of spectral swapping [21–23, 25–27]. This phenomenon involves the interchange of spectra between $\nu_e(\bar{\nu}_e)$ and $\nu_x(\bar{\nu}_x)$ across a range of neutrino energies.

However, further exploration revealed that the actual FC scenarios within more realistic supernova models can be considerably diverse. For example, studies have demonstrated the existence of fast flavor conversions (FFCs) when the angular distributions of ν_e and $\bar{\nu}_e$ exhibit significant enough differences, so that they can cross each other [28–30] (see [4] for a review on flavor mechanisms).

Additionally, in the presence of strong magnetic fields, (partial) flavor equilibration between neutrinos and antineutrinos may occur due to the presence of the neutrino magnetic moment [31–33]. Another interesting FC scenario occurs when neutrinos can experience non-standard self interactions (NSSI). Such NSSI introduce yet another facet of flavor equilibration among various neutrino (antineutrino) flavors [34, 35].

In this paper, we utilize Bayesian inference techniques to discern between various neutrino FC scenarios by analyzing a future SN neutrino signal. Our specific focus lies within the SN accretion phase, characterized by distinctive energy spectra among different neutrino species. We demonstrate that a sufficiently large number of neutrino events significantly enhances the likelihood of distinguishing between different FC scenarios in the SN environment.

The paper is structured as follows. In Sec. II, we describe the SN neutrino spectra. We then discuss the neutrino FC scenarios in Sec. III. Sec. IV introduces the neutrino detection channels we consider in this study. Before concluding in Sec. VI, we present the results of our Bayesian analysis of a prospective SN neutrino signal in

Sec. V.

II. SN NEUTRINO SIGNAL

To ensure the maximum impact of the FC on neutrino energy spectra, we strategically select the SN accretion phase, anticipating the greatest disparity between different neutrino spectra. As a first step, we make the simplifying hypothesis that the neutrino spectral parameters are stationary during the emission of the neutrino signal. This assumption can be justified on the basis of two key factors. Firstly, during the SN accretion phase, the neutrino spectral parameters can reasonably be considered constant, at least for several tens of milliseconds, probably allowing for the accumulation of a sufficient number of events. Additionally, our methodology allows us to determine the minimum time interval for which the spectral parameters should remain constant to obtain any conclusive result.

In scenarios where neutrino FC is not present, the time-integrated neutrino energy-differential number flux of a specific neutrino species, ν_β , at a distance D from the SN can be written as [24],

$$\mathcal{F}_{\nu_\beta}(E_\nu) = \frac{\mathcal{E}_{\nu_\beta}}{4\pi D^2 \langle E_{\nu_\beta} \rangle} f_{\nu_\beta}(E_\nu) \quad (1)$$

with

$$f_{\nu_\beta}(E_\nu) = \frac{1}{T_{\nu_\beta} \Gamma(1 + \alpha_{\nu_\beta})} \left(\frac{E_\nu}{T_{\nu_\beta}} \right)^{\alpha_{\nu_\beta}} \exp(-E_\nu/T_{\nu_\beta}) \quad (2)$$

being the normalized ν_β spectrum, where E_ν is the neutrino energy. Here, α_{ν_β} and $\langle E_{\nu_\beta} \rangle$ are the pinching parameter and the average neutrino energy, the parameters which describe the normalized spectrum and $T_{\nu_\beta} = \langle E_{\nu_\beta} \rangle / (1 + \alpha_{\nu_\beta})$. In addition, \mathcal{E}_{ν_β} is the time-integrated neutrino luminosity for the time interval of interest, i.e., $\mathcal{E}_{\nu_\beta} = \int_t^{t+\Delta t} dt L_{\nu_\beta}(t)$, with L_{ν_β} being the neutrino luminosity.

TABLE I. The neutrino energy spectra we consider in this study, relevant to the SN accretion phase. While the LSD spectrum shows significant variations among neutrino species, in the SSD one the spectral variations are less prominent [36, 37].

LSD
$\mathcal{E}_{\nu_e} : \mathcal{E}_{\bar{\nu}_e} : \mathcal{E}_{\nu_x} = 1 : 1 : 0.33$
$\langle E_{\nu_e} \rangle : \langle E_{\bar{\nu}_e} \rangle : \langle E_{\nu_x} \rangle = 9 : 12 : 16.5$
$\alpha_{\nu_e} : \alpha_{\bar{\nu}_e} : \alpha_{\nu_x} = 3.2 : 4.5 : 2.3$
SSD
$\mathcal{E}_{\nu_e} : \mathcal{E}_{\bar{\nu}_e} : \mathcal{E}_{\nu_x} = 1 : 1 : 0.75$
$\langle E_{\nu_e} \rangle : \langle E_{\bar{\nu}_e} \rangle : \langle E_{\nu_x} \rangle = 9 : 12 : 14$
$\alpha_{\nu_e} : \alpha_{\bar{\nu}_e} : \alpha_{\nu_x} = 3.26 : 4.76 : 2.26$

In the following, we analyze two distinctive neutrino energy spectra relevant to the SN accretion phase, as described in Table. I: one with large spectral difference (LSD), showing significant variations among neutrino species, and another with small spectral difference (SSD), where spectral variations are less prominent. Here, we make the assumption that ν_x and $\bar{\nu}_x$ have identical spectral shapes. Also note that the average energies are in MeV, and that there is no unit in front of \mathcal{E} , given that we here consider the scenario where the number of observed neutrino event are fixed (see the next section for more details). While the latter profile is more suitable for SN models with lighter progenitors, the former is more appropriate for models involving heavier ones [36, 37].

III. NEUTRINO FLAVOR CONVERSION SCENARIOS

In this section, we briefly describe the FC mechanisms under consideration. It is important to highlight that apart from the conventional MSW mechanism, all the FC scenarios we explore stem from coherent neutrino-neutrino scatterings (mean-field approximation). As a result, the total number of (anti)neutrinos within a designated energy/momentum range remains conserved.

To provide the reader with an impression of the various FC scenarios, Fig. 1 displays the initial spectra of $\bar{\nu}_e$ and $\bar{\nu}_x$ derived from the LSD profile, alongside the resulting $\bar{\nu}_e$ spectrum post the given FC scenario.

A. No flavor conversions (NFC)

In our first example, we examine the FC scenario where the emitted neutrino fluxes within the SN core precisely translates to larger distances without alteration. This scenario serves as a benchmark for comparison. Surprisingly, while seemingly idealistic, this scenario is not entirely implausible, given the fact we do not yet know to which extent FC in the SN core influences the SN neutrino fluxes.

B. MSW effect

The established MSW mechanism stands as one of the most extensively explored neutrino FC mechanisms. It occurs due to a resonant behavior generated by a cancellation in the diagonal term of the Hamiltonian, between the matter and vacuum components. This effect is highly sensitive to the neutrino mass hierarchy. Vacuum neutrino oscillation experiments provide accurate knowledge of mass-squared differences. Due to matter effects in the Sun, we also know that $\Delta m_{21}^2 > 0$. However, the sign of the atmospheric mass splitting, Δm_{31}^2 , is currently unknown since current measurement solely revealing its

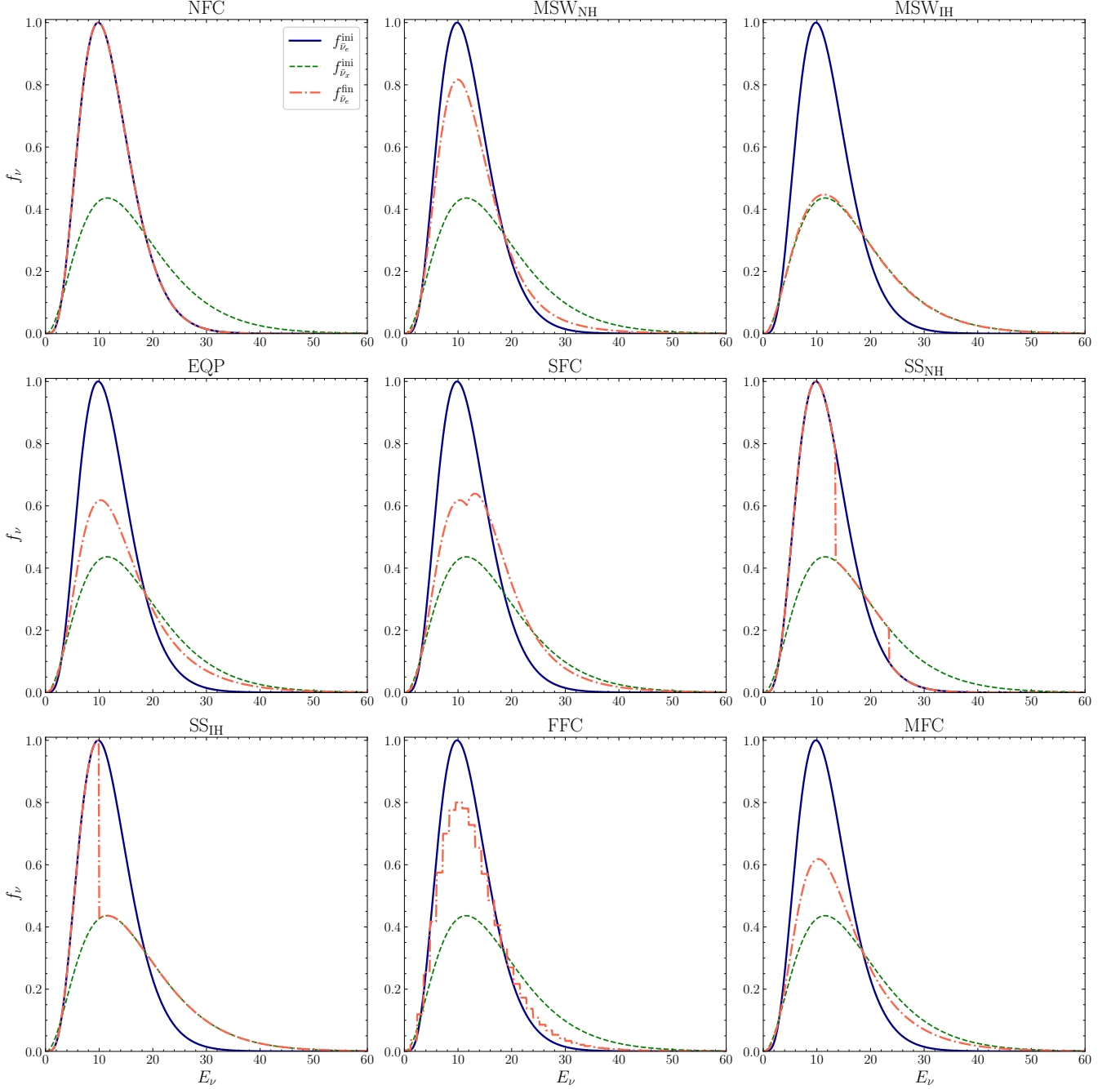


FIG. 1. Initial spectra of $\bar{\nu}_e$ and $\bar{\nu}_x$ (derived from the LSD profile), as well as the resulting $\bar{\nu}_e$ spectrum post FC for different FC scenarios. Here, the initial spectra (LSD) are assumed to exist at the neutrinosphere. Then, we have applied the FC scenarios (defined in Sec. III) given in the title of each panel.

absolute value. Hence, we can have either a normal hierarchy (NH) with $\Delta m_{31}^2 > 0$, or an inverted hierarchy (IH) with $\Delta m_{31}^2 < 0$. Assuming a perfect adiabatic MSW, in

NH one has [38],

$$\begin{aligned}
 \mathcal{F}_{\nu_e} &= \sin^2 \theta_{13} \mathcal{F}_{\nu_e}^0 + \cos^2 \theta_{13} \mathcal{F}_{\nu_x}^0, \\
 \mathcal{F}_{\bar{\nu}_e} &= \cos^2 \theta_{12} \cos^2 \theta_{13} \mathcal{F}_{\bar{\nu}_e}^0 + (1 - \cos^2 \theta_{12} \cos^2 \theta_{13}) \mathcal{F}_{\bar{\nu}_x}^0, \\
 2\mathcal{F}_{\nu_x} &= \cos^2 \theta_{13} \mathcal{F}_{\nu_e}^0 + (1 + \sin^2 \theta_{13}) \mathcal{F}_{\nu_x}^0, \\
 2\mathcal{F}_{\bar{\nu}_x} &= (1 - \cos^2 \theta_{13} \cos^2 \theta_{12}) \mathcal{F}_{\bar{\nu}_e}^0 + (1 + \cos^2 \theta_{13} \cos^2 \theta_{12}) \mathcal{F}_{\bar{\nu}_x}^0,
 \end{aligned} \tag{3}$$

while for IH, it is given by,

$$\begin{aligned}\mathcal{F}_{\nu_e} &= \cos^2 \theta_{13} \sin^2 \theta_{12} \mathcal{F}_{\nu_e}^0 + (1 - \sin^2 \theta_{12} \cos^2 \theta_{13}) \mathcal{F}_{\nu_x}^0, \\ \mathcal{F}_{\bar{\nu}_e} &= \sin^2 \theta_{13} \mathcal{F}_{\bar{\nu}_e}^0 + \cos^2 \theta_{13} \mathcal{F}_{\bar{\nu}_x}^0, \\ 2\mathcal{F}_{\nu_x} &= (1 - \cos^2 \theta_{13} \sin^2 \theta_{12}) \mathcal{F}_{\nu_e}^0 + (1 + \sin^2 \theta_{12} \cos^2 \theta_{13}) \mathcal{F}_{\nu_x}^0, \\ 2\mathcal{F}_{\bar{\nu}_x} &= \cos^2 \theta_{13} \mathcal{F}_{\bar{\nu}_e}^0 + (1 + \sin^2 \theta_{13}) \mathcal{F}_{\bar{\nu}_x}^0.\end{aligned}\quad (4)$$

Here \mathcal{F}_ν^0 denotes the neutrino fluxes at the neutri-nosphere before flavor conversion mechanisms produce spectral distortions.

C. Spectral swapping (SS)

The initial investigations into collective neutrino oscillations within the SN environment focused on simplified symmetric models, such as the stationary spherically symmetric neutrino bulb model. These studies revealed a significant phenomenon: spectral swapping phenomenon which involves the swapping of spectra between $\nu_e(\bar{\nu}_e)$ and $\nu_x(\bar{\nu}_x)$ over a range of neutrino energies, due to the collective oscillations of SN neutrinos [4, 21–23, 25, 27]. Though this was first observed in stationary spherically symmetric models, in Ref. [39] the authors showed that SS can also exist in multi-dimensional models provided that FCs do not occur very deep inside the SN core.

The spectral swap can occur around the neutrino energies where there is a zero crossing in the energy spectrum defined as,

$$g_\omega = \frac{|\Delta m^2|}{2\omega^2} \begin{cases} \mathcal{F}_{\nu_e}^0 - \mathcal{F}_{\nu_x}^0 & (\omega > 0) \\ \mathcal{F}_{\bar{\nu}_x}^0 - \mathcal{F}_{\bar{\nu}_e}^0 & (\omega < 0) \end{cases} \quad (5)$$

where $\omega = \frac{|\Delta m^2|}{2E_\nu}$ and $|\Delta m^2|$ is the neutrino mass squared difference. Note that there can be a crossing (by default) when $\omega \rightarrow 0$, corresponding to $E_\nu \rightarrow \infty$, which if unstable leads to an SS for the tail of the energy spectra.

The spectral crossings exhibit instability in the IH (NH) scenarios when the crossing slope is positive (negative), resulting in a swap across a finite range of ω . While zero crossings in g_ω serve as a criterion for instability concerning SS, determining the swapping width is not straightforward. In practice, there might exist even crossings that do not induce any spectral swapping.

In our computations, we prioritize practicality over ambition when estimating the width of the SS. Specifically, if the crossing at $\omega = 0$ is unstable, we approximate $\Delta\omega \simeq 0.7 \text{ km}^{-1}$. Alternatively, for each crossing, we assume that SS occurs within $\Delta E_\nu = \pm 7.5 \text{ MeV}$. These assumptions align with the simulation results [21, 25]. Furthermore, we have verified that the width of the crossings, if sufficiently large, does not impact the results presented in the subsequent section.

D. Slow flavor conversions (SFC)

In the context of slow modes, in some symmetric models like the bulb model, it has been shown that some flavor equilibration can be reached [40]. Such equilibrium leads to neutrino flavor equipartition up to the constraint of neutrino electron lepton number conservation. The resulted neutrino spectra can then be found as,

$$\begin{aligned}\mathcal{F}_{\nu_e} &= \mathcal{F}_{\text{eq}} + \max(0, \mathcal{L}), \\ \mathcal{F}_{\bar{\nu}_e} &= \mathcal{F}_{\text{eq}} + \max(0, -\mathcal{L}), \\ \mathcal{F}_{\nu_x} &= \mathcal{F}_{\bar{\nu}_x} = \mathcal{F}_{\text{eq}},\end{aligned}\quad (6)$$

where \mathcal{F}_{eq} is the equilibrium \mathcal{F} , defined by,

$$\mathcal{F}_{\text{eq}} = \begin{cases} \frac{1}{3}(\mathcal{F}_{\bar{\nu}_e}^0 + 2\mathcal{F}_{\bar{\nu}_x}^0), & \text{if } \mathcal{L} > 0, \\ \frac{1}{3}(\mathcal{F}_{\nu_e}^0 + 2\mathcal{F}_{\nu_x}^0), & \text{if } \mathcal{L} \leq 0. \end{cases} \quad (7)$$

where $\mathcal{L} = \mathcal{F}_{\nu_e}^0 - \mathcal{F}_{\bar{\nu}_e}^0$, provides information on the neutrino electron lepton number. For more details on the SFC prescription, we refer an interested reader to Ref. [41, 42].

E. Fast flavor conversions (FFC)

One of the most recent developments in the field of neutrino FC in the SN environment has been the discovery of FFCs [43–45]. The assessment of the outcomes of FFCs has been extensively explored through localized dynamical simulations conducted within confined spaces using periodic boundary conditions [46–57]. Insights obtained from these investigations reveal a tendency toward kinematic decoherence during flavor conversions, leading to the emergence of quasistationary states. These stable states can be characterized by survival probabilities, governed by the conservation of neutrino lepton number, and have shown potential for accurate analytical modeling [57].

In this study, we take the analytical survival probability developed in Ref. [57], assuming an axisymmetric neutrino angular distributions. In addition, we assumed the maximum entropy angular distribution [58], defined as,

$$\mathcal{G}_\nu(\mu) = \exp(\eta + a\mu), \quad (8)$$

where η and a are some arbitrary parameters and $\mu = \cos \theta_\nu$, with θ_ν being the zenith angle of the neutrino velocity, and,

$$\mathcal{G}_\nu(\mu) = \int_0^\infty \int_0^{2\pi} \frac{E_\nu^2 dE_\nu d\phi_\nu}{(2\pi)^3} \mathcal{G}_\nu(\mathbf{p}), \quad (9)$$

where $\mathcal{G}_\nu(\mathbf{p})$'s are the neutrino occupation numbers of different flavors. Here, ϕ_ν is the azimuthal angle of the neutrino velocity. If one is then provided with the flux factors of the energy-integrated as well as those of each

energy bin, one can find the outcome of FFC for each energy bin. Here, the flux factor is defined as,

$$\mathbf{F}_\nu = \frac{I_1}{I_0} \quad (10)$$

where I 's are the radial moments of the neutrino angular distributions, defined as,

$$I_n = \int_{-1}^1 d\mu \mu^n \int_0^\infty \int_0^{2\pi} \frac{E_\nu^2 dE_\nu d\phi_\nu}{(2\pi)^3} \mathcal{G}_\nu(\mathbf{p}), \quad (11)$$

for the energy-integrated moments, and as,

$$I_{n,i} = \frac{E_{\nu,i}^2 \Delta E_{\nu,i}}{(2\pi)^3} \int_{-1}^1 d\mu \mu^n \int_0^{2\pi} d\phi_\nu \mathcal{G}_\nu(\mathbf{p}), \quad (12)$$

when the corresponding quantities for each energy bin are required. Here, $E_{\nu,i}$ and $\Delta E_{\nu,i}$ are the mean energy and the width of the i -th energy bin. For the the energy-integrated flux factors, we take: $\mathbf{F}_{\nu_e} = 0.5$, $\mathbf{F}_{\bar{\nu}_e} = 0.7$, and $\mathbf{F}_{\nu_x} = 0.8$. Then for each energy bin we adopted an assumption describing the relationship as $\mathbf{F}_{\nu,i} = \mathbf{F}_\nu (70 - E_{\nu,i})^2/60^2$. Here, we have assumed that the spectra approach zero for $E_{\nu,i} \gtrsim 60$ MeV. Note that it is anticipated that the flux factor will decrease with increasing neutrino energy, and this reduction is expected to be nonlinear, due to the nonlinear scaling of the neutrino scattering cross-section (with the matter) with neutrino energy in the SN environment. While our assumption regarding the dependence of the flux factor on energy is speculative, it aligns with both of these anticipated conditions. Otherwise, we regard this assumption as an initial exploration, considering it as the first stage of such a study. Further investigations may involve exploring alternative formulations for the energy dependence of the flux factor.

F. Neutrino flavor equipartition (EQP)

The existence of neutrino non-standard self-interactions (NSSI) has been established as a mechanism capable of inducing equipartition between neutrinos and antineutrinos separately [34], given by,

$$\begin{aligned} \mathcal{F}_{\nu_e} &= \mathcal{F}_{\nu_x} = \frac{1}{3}(\mathcal{F}_{\nu_e}^0 + 2\mathcal{F}_{\nu_x}^0), \\ \mathcal{F}_{\bar{\nu}_e} &= \mathcal{F}_{\bar{\nu}_x} = \frac{1}{3}(\mathcal{F}_{\bar{\nu}_e}^0 + 2\mathcal{F}_{\bar{\nu}_x}^0). \end{aligned} \quad (13)$$

This phenomenon occurs due to the introduction of non-standard off-diagonal terms in the neutrino-neutrino interaction Hamiltonian, resulting in the emergence of unavoidable neutrino flavor instabilities. These instabilities subsequently trigger flavor decoherence, ultimately leading to a state of flavor equipartition within both the neutrino and antineutrino sectors.

In several beyond Standard Model (BSM) theories of particle physics [59, 60], such neutrino NSSIs are permitted. These interactions are facilitated through a vector mediator, which modifies the effective Lagrangian

to $\mathcal{L}_{\text{eff}} \supset G_F[\mathbf{G}^{\alpha\beta}\bar{\nu}_\alpha\gamma^\mu\nu_\beta][\mathbf{G}^{\xi\eta}\bar{\nu}_\xi\gamma^\mu\nu_\eta]$. This revised Lagrangian closely resembles the neutrino-neutrino interaction Lagrangian of the Standard Model (SM), but now introduces new interaction terms that couple neutrinos of different flavors via $\mathbf{G}^{\alpha\beta}$'s.

G. Magnetically-induced flavor conversion (MFC)

Neutrinos, which possess exceedingly small yet non-zero magnetic moments (see Refs. [61–63] for an in-depth review), can exhibit modified flavor evolution when exposed to external magnetic fields. This effect becomes particularly pronounced in environments with ultra-strong magnetic fields (exceeding 10^{15} Gauss), such as neutron star mergers and magneto-rotational CC-SNe [64]. These extreme conditions present ideal scenarios for investigating the interplay between neutrinos and magnetic fields and their impact on collective neutrino oscillations. For example for Majorana neutrinos, the introduction of a magnetic term can induce neutrino-antineutrino oscillations.

Recent studies have highlighted the potential significance of the magnetic term when it reaches a comparable magnitude to other terms in the Hamiltonian. Here we follow Refs. [31–33] that have found an equipartition among ν_e ($\bar{\nu}_e$) and ν_x ($\bar{\nu}_x$) when the contribution coming from the neutrino magnetic moment to the neutrino Hamiltonian becomes as sizeable as the other terms, described by:

$$\begin{aligned} \mathcal{F}_{\nu_e} &= \mathcal{F}_{\bar{\nu}_x} = \frac{1}{3}(\mathcal{F}_{\nu_e}^0 + 2\mathcal{F}_{\bar{\nu}_x}^0), \\ \mathcal{F}_{\bar{\nu}_e} &= \mathcal{F}_{\nu_x} = \frac{1}{3}(\mathcal{F}_{\bar{\nu}_e}^0 + 2\mathcal{F}_{\nu_x}^0). \end{aligned} \quad (14)$$

IV. NEUTRINO CROSS SECTIONS

Before discussing the outcomes of our statistical analysis, let us first briefly outline the neutrino detection channels under consideration in our study. In our statistical analysis, we consider neutrino events as can be seen by water Cherenkov detectors, namely Super-Kamiokande and Hyper-Kamiokande [65, 66]. In particular, we take inverse beta decay (IBD) and neutrino elastic scattering on electrons (ES) as the relevant processes ¹.

In this study, we build upon our previous works outlined in Refs. [8, 9, 11] (see these References for further details and for the neutrino cross sections). In particular, in our calculations, we work under the assumptions of a 100% detector efficiency and the absence of background events. We also ignore the possible existence of a time

¹ Note that there are a range of other possibilities for neutrino detection which are beyond the scope of this work and we leave them for a future study.

offset between the start of neutrino emission and the detection of the first event. These considerations are made to determine the very minimum number of events necessary to derive conclusive results. The energy-differential rate for the reaction j generated by the neutrino species ν_β can be calculated as,

$$\frac{dN_{\nu_\beta,j}}{dE} = n_{T,j} \int_{E_{th}}^{\infty} dE_\nu \mathcal{F}_{\nu_\beta}(E_\nu) \sigma_{\nu_\beta,j}(E_\nu) \quad (15)$$

where E_{th} is the neutrino energy threshold for each process, $n_{T,j}$ is the number of targets for the process j , and $\sigma_{\nu_\beta,j}(E_\nu)$ is the energy dependent cross section for a given reaction and species.

For the IBD events, we use the analytical formula developed in Ref. [67],

$$\sigma_{IBD} \simeq 10^{-43} \text{cm}^2 p_e E_e E_\nu^x, \quad (16)$$

with $x = -0.07056 + 0.02018 \ln E_\nu - 0.001953 \ln^3 E_\nu$ and $E_e \simeq E_\nu - \Delta$, with $\Delta \simeq 1.293 \text{ MeV}$. For the ES channel, we use tree level expression of the cross section [68, 69]:

$$\frac{d\sigma_{\nu_\beta,ES}}{dy} = \frac{2G_F^2 m_e E_\nu}{\pi} \left[g_{\nu_\beta}^2 + g_{\nu_\beta}^{\prime 2} (1-y)^2 - g_{\nu_\beta} g_{\nu_\beta}' \frac{m_e}{E_\nu} y \right] \quad (17)$$

where g and g' can be obtained using the Weinberg weak-mixing angle and are different for different neutrino species (see Table. 3 of Ref. [9]), G_F is the Fermi constant, and m_e is the electron mass. Here, y is the electron kinetic energy, $K_e = E_e - m_e$, divided by the neutrino energy, for which $0 < y = K_e/E_\nu < (1 + m_e/2E_\nu)^{-1}$.

In Fig. 2, we present an illustrative event rate distribution given our equipartition FC prescription, provided both for the IBD and ES detection channels. It is important to note that the anticipated total number of ES events is expected not to exceed a few percent of the IBD events.

V. BAYESIAN ANALYSIS OF THE SUPERNOVA NEUTRINO EVENTS

In this section, we provide the results of our Bayesian analysis to differentiate neutrino FC scenarios via a future SN neutrino signal. For a specific FC scenario, M_a , an event with an energy E_i has the probability distribution:

$$p(E_i|M_a) = \frac{1}{\langle N \rangle} \frac{dN}{dE}, \quad (18)$$

where dN/dE can be found using Eq. (15) for each case of FC considered, and $\langle N \rangle = \int_{E_{th}}^{\infty} dE (dN/dE)$ is the expected total number of events.

One can then find the likelihood of observing a set of events with energies $\{E_i\}$ for i in $(1, 2, \dots, N_{\text{obs}})$ as,

$$P(\{E_i\}|M_a) = \prod_{i=1}^{N_{\text{obs}}} p(E_i|M_a), \quad (19)$$

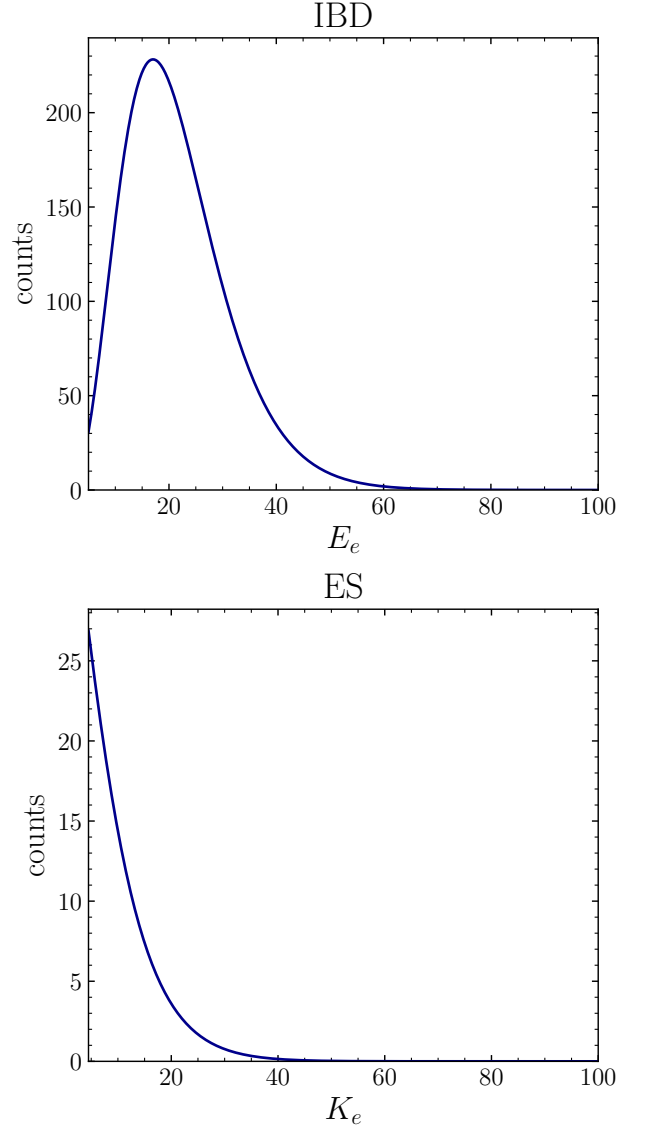


FIG. 2. Event rate distributions for the IBD and ES detection channels, as a function of the electron total and kinetic energies, E_e and K_e , respectively. Here, the EQP FC scenario is employed.

where N_{obs} is the observed number of neutrino events. In our calculation, we derive N_{obs} events using Eq. (15). We then calculate the likelihood of observing a set of events with energies $\{E_i\}$ using the above equation.

Assuming that the different FC scenarios have the same priors, one can then find the Bayes factor,

$$\text{BF}_{10} = \frac{P(\{E_i\}|M_1)}{P(\{E_i\}|M_0)}, \quad (20)$$

where M_0 represents the null hypothesis, which is the model the events are generated with, and M_1 is the alternative hypothesis to be compared with the null hypothesis. The guidelines for interpreting the natural logarithm of BF_{10} are as follows: i) $\ln \text{BF}_{10} \in (0-1)$: Not signifi-

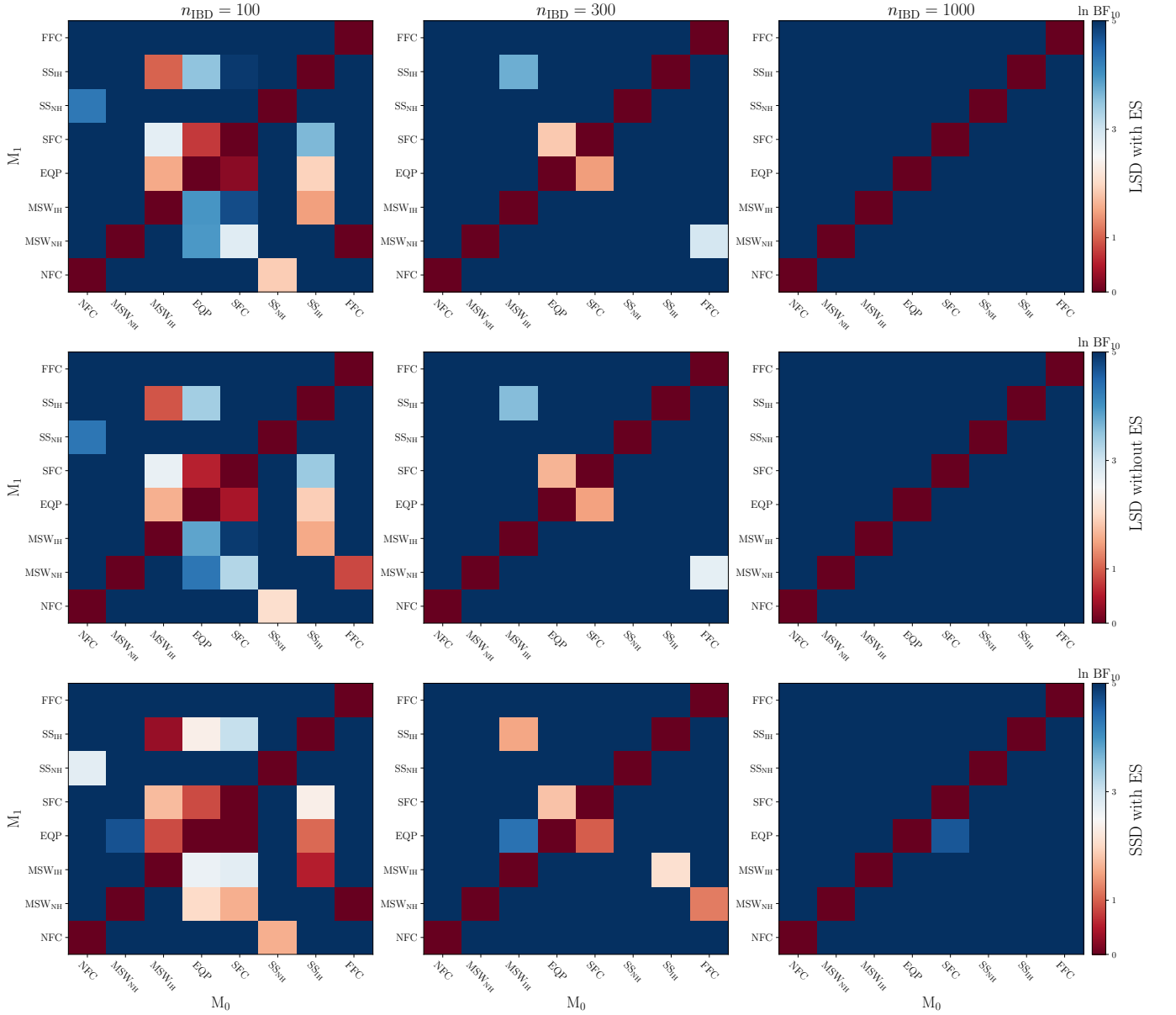


FIG. 3. Bayes factor comparison among various FC scenarios across different observed neutrino events, $N_{\text{obs}} = 100, 300$, and 1000. The x-axis denotes the null hypothesis, representing the model by which the neutrino events were generated, while the y-axis corresponds to the alternative hypothesis. Here, the diagonal values are by default set to zero. The upper panels show the results using the LSD spectrum, incorporating both the IBD and ES detection channels. In the middle panels, we present the Bayes factor calculations similar to the upper panels, but excluding the ES channel. The lower panels exhibit the Bayes factor values derived from the SSD spectrum calculations (including both IBD and ES channels).

cant, ii) $\ln BF_{10} \in (1-3)$: Indicates a positive evidence, iii) $\ln BF_{10} \in (3-5)$: Reflects strong evidence, and iv) $\ln BF_{10} > 5$: Demonstrates very strong evidence.

In line with Ref. [15], our analysis revolves around a fixed number of observed neutrino events, irrespective of the absolute SN neutrino luminosities and its distance from the detector. In this context, the absolute neutrino luminosities of the SN and its distance from the detector become irrelevant in our evaluations, i.e., they can not

be considered as free parameters. This is because, in any case, specific values for these parameters must be assumed to obtain the given number of events for each FC scenario under consideration. What is important in our analysis are the spectral parameters and the relationship between the luminosities of various neutrino species.

We consider calculations in which the number of observed events are 100, 300, and 1000. In addition, in our calculations, we assume a constant ratio between the

number of observed events in the IBD and ES channels, namely $N_{\text{ES}} = 0.05 N_{\text{IBD}}$, consistent with the expectations in a water Cherenkov detector.

A. Analysis assuming known spectral parameters

In our first evaluation of the differentiating between various FC scenarios, we work under the assumption that the spectral parameters are known, essential for calculating the likelihoods outlined in Eqs. (19) and (20). This assumption stands on two grounds. Firstly, it offers an initial estimation of our capability of differentiating between various FC scenarios. Should the FC models remain indistinguishable given the spectral parameters, discerning them in situations requiring optimisation for obtaining spectral parameters (as discussed in the following section) becomes a considerable challenge. Moreover, it is plausible to consider the availability of such spectral information, particularly in models tied to specific progenitors once multi-dimensional simulations by different groups will reach convergence. Nevertheless, these preliminary calculations yield crucial initial insights that prove invaluable later in the analysis.

In Fig. 3, we present the Bayes factor obtained from Eq.(20) across various FC scenarios, given the spectral parameters. The results are shown for $N_{\text{obs}} = 100, 300$, and 1000. The upper panels illustrate outcomes derived from events generated using the LSD spectrum, with more pronounced differences among neutrino spectra, where we have considered both the IBD and ES detection channels. Our approach involves running 1000 Monte Carlo (MC) simulations for each scenario, subsequently averaging the results to obtain the Bayes factor's average.

Let us make a few remarks. Firstly, even with $N_{\text{obs}} = 100$, discerning certain FC models becomes feasible. However, a larger event count significantly enhances our ability to differentiate between the FC scenarios. Then upon reaching $N_{\text{obs}} = 1000$, perfect differentiation among all the FC models becomes achievable. It is also illuminating to note that in these calculations, we have not considered the MFC scenario, since ν_x and $\bar{\nu}_x$ are indistinguishable observationally, MFC behaves closely to that of the EQP scenario.

To provide the reader with some insight into the Bayes factor values, Table II presents $\ln \text{BF}_{10}$ corresponding to the LSD calculation with $N_{\text{obs}} = 300$. It is important to note that several computations exhibit clear distinguishability among FC scenarios. However, certain entries in the table display values below 10, suggesting a potential lack of strong differentiation when considering the whole range of MC calculations. In specific cases, the samples with the most adverse impact on the Bayes factor might reduce $\ln \text{BF}_{10}$ value to less than 5.

In the middle panels of Fig. 3, we display the Bayes factor for the calculations closely resembling those in the upper panel with the LSD spectrum, except for the ex-

	NFC	MSW _{NH}	MSW _{IH}	EQP	SFC	SS _{NH}	SS _{IH}	FFC
NFC		78.8	287.9	191.8	165.5	10.8	274.2	44.5
MSW _{NH}	40.0		46.0	15.8	13.0	42.5	41.4	2.9
MSW _{IH}	161.5	51.0		9.4	12.3	148.3	5.2	65.7
EQP	99.0	17.9	7.1		1.4	93.3	7.6	28.2
SFC	95.3	17.2	10.5	1.8		89.1	12.7	25.3
SS _{NH}	12.1	82.1	279.2	188.1	161.4		265.4	48.2
SS _{IH}	149.2	45.5	3.7	9.4	14.1	135.3		60.6
FFC	29.7	195.3	532.9	395.6	334.4	32.7	531.9	

TABLE II. $\ln \text{BF}_{10}$ values corresponding to the LSD calculation with $N_{\text{obs}} = 300$ (the upper middle panel of Fig. 3). The rows/columns indicate the null/alternative hypotheses. The red cells show the values below 5. Note that several cells show clear distinguishability among FC models. However, certain entries in the table display values below 10, suggesting a potential lack of strong differentiation when considering the whole range of MC calculations.

clusion of the ES channel. It is important to note the minimal discrepancy between the upper and middle panels, indicating that the primary influential factor here is the number of observed neutrino events. The ES channel, while included in the calculations of the upper panel, appears to play a subdominant role and does not significantly impact the outcomes.

In the lower panels of Fig. 3, the Bayes factor for the SSD spectrum calculations is displayed, revealing more subtle variations across the neutrino spectra. Comparatively, the distribution of the Bayes factor appears less prominent than in the middle and upper panels. However, large values of $\ln \text{BF}_{10}$ can still be observed and most of the FC scenarios can be distinguished well from each other. This suggests that even in less favorable scenarios, there remains strong potential for discerning between different FC scenarios.

B. FC scenarios, including the MSW effect

In the preceding part, we focused on a single FC scenario. However and in practice, neutrinos are expected to undergo the MSW effect after encountering FC mechanisms in the deeper SN zones. Hence, it follows that each FC scenario should encompass an MSW effect on top, either within the NH or IH paradigm. In our computations, we consider various FC scenarios, and the final neutrino fluxes which are detailed in Sec.III. Given that the MSW effect is expected to occur far from other FC scenarios, we proceed by assuming that the MSW effect can be superimposed. In this context, we consider the final \mathcal{F}_ν post FC scenario as an input (\mathcal{F}_ν^0) to Eqs.(3) and (4), accounting for the MSW effect.

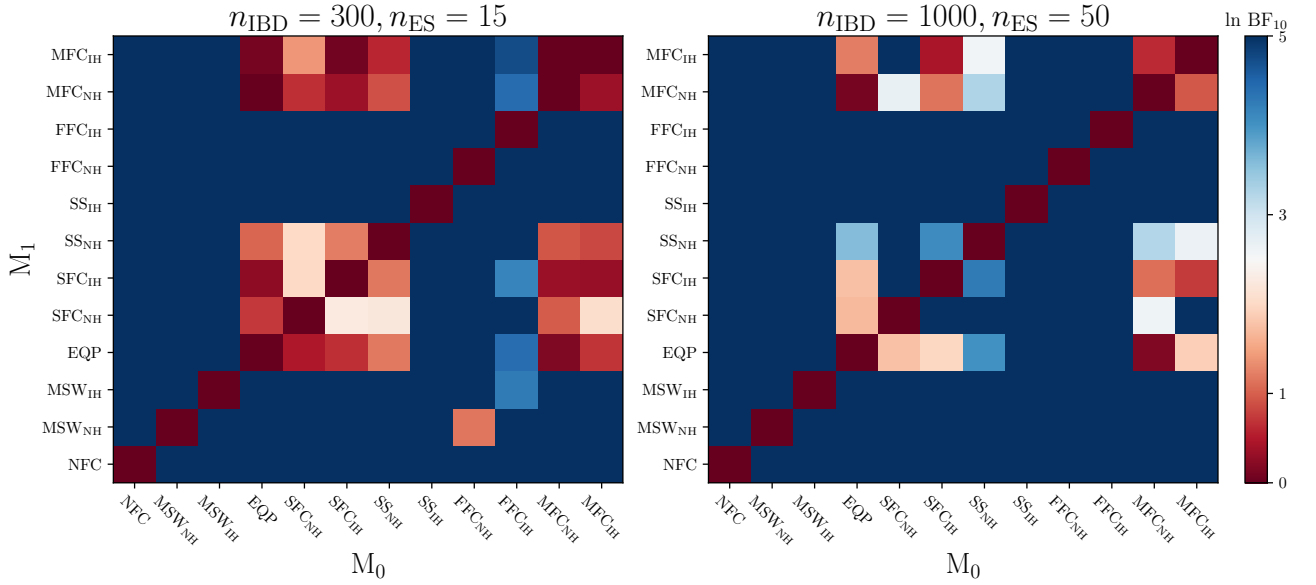


FIG. 4. The Bayes factor regarding FC scenarios with MSW. Note that here we have considered the LSD spectrum and known spectral parameters. The x-axis denotes the null hypothesis, representing the model by which the neutrino events were generated, while the y-axis corresponds to the alternative hypothesis. The diagonal values are by default set to zero.

In Fig. 4, we illustrate the Bayes factor regarding FC scenarios with MSW. In this context, we have considered the LSD spectrum assuming known spectral parameters, as above, and with $N_{\text{obs}} = 300$ and 1000 . It is evident that the introduction of FC scenarios with MSW on top amplifies the degeneracy, thereby complicating the distinction between different FC scenarios. Note that the EQP scenario does not include any MSW on top, since the existing equipartition is already blind to MSW effect.

C. Unknown spectral parameters

Up to this point, our approach involved assuming that the spectral parameters were known once the Bayes factor was calculated. However, in reality, the Bayes factor remains unknown at the time of detection. As a result, one should first optimize over the likelihood distribution to determine the most probable spectral parameters. In Fig. 5, we show our findings in such a scenario. In our computations, we initially optimized the likelihood for each model, obtaining the optimal spectral parameters and subsequently, we calculated the likelihood for each FC scenario. During the optimization process, we assume the spectral parameters to be confined in the following intervals:

$$\begin{aligned}
 &L_{\bar{\nu}_e}/L_{\nu_e}, L_{\nu_x}/L_{\nu_e} \in (0.1, 1.5), \\
 &\langle E_{\nu_e} \rangle \in (5, 15), \langle E_{\bar{\nu}_e} \rangle \in (8, 18), \langle E_{\nu_x} \rangle \in (10, 20) \text{ MeV}, \\
 &\alpha_{\nu_e} \in (2.5, 4), \alpha_{\bar{\nu}_e} \in (3.5, 5), \alpha_{\nu_x} \in (1.5, 3),
 \end{aligned}
 \tag{21}$$

which could be considered conservative enough for the SN accretion phase. To generate the neutrino signal for each model, we utilized the LSD spectrum in these calculations. In addition, being guided by the results in the previous section, we only consider the IBD detection channel to enhance the computation efficiency.

When spectral parameters remain unknown, distinguishing between various FC scenarios becomes notably challenging, necessitating a larger number of observed neutrino events. However and despite this complexity, there remains optimism regarding the possibility of distinguishing between different FC scenarios.

In our current study, we have focused on N_{obs} values up to 1000. However, it is plausible to extend this analysis to encompass a larger number of neutrino events during the SN accretion phase, especially when incorporating the Hyper-Kamiokande or/and the inclusion of multiple detectors is considered. In Fig. 6, we present calculations where $N_{\text{obs}} = 10000$. This expanded dataset distinctly separates a larger number of FC scenarios, showing their discernibility from one another.

VI. DISCUSSION AND OUTLOOK

Neutrino FC within the SN environment is an intricate and multifaceted phenomenon. Previous studies have shown that varying physics within the SNe can yield diverse FC scenarios affecting neutrino flavor evolution in these extreme settings. In this study we have employed Bayesian techniques to discern and differentiate between various FC scenarios in the SN environment us-

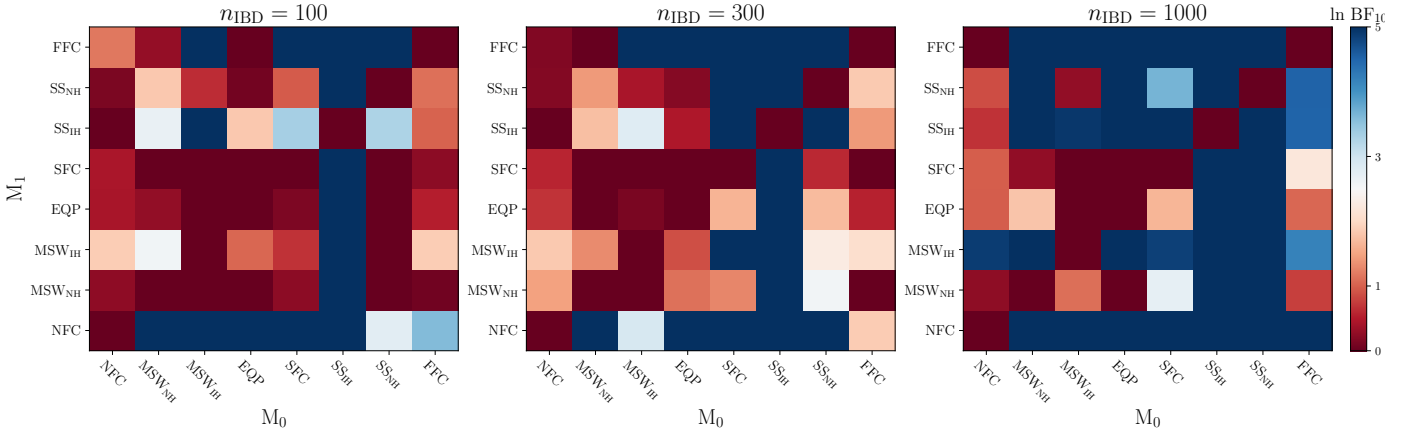


FIG. 5. The Bayes factor regarding the case where the spectral parameters are not known beforehand. The x-axis denotes the null hypothesis (obtained from the LSD spectrum), representing the model by which the neutrino events were generated, while the y-axis corresponds to the alternative hypothesis. The diagonal values are by default set to zero.

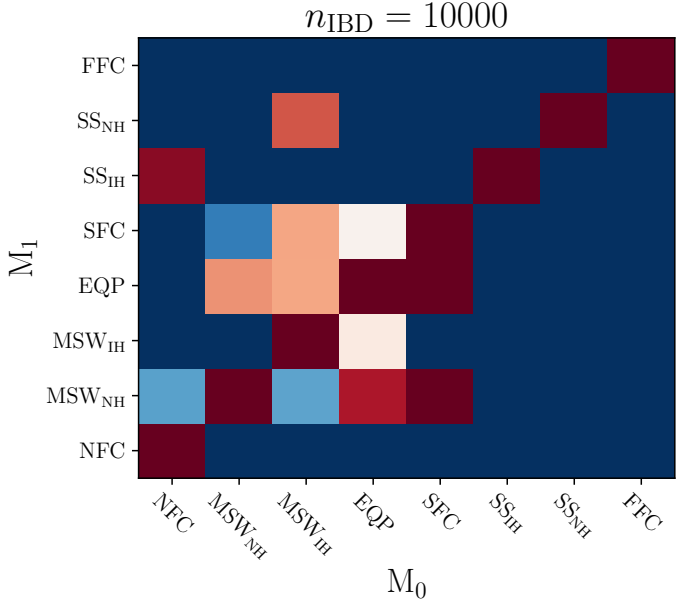


FIG. 6. The Bayes factor regarding the case where the spectral parameters are unknown, with $n_{\text{IBD}} = 10000$. The x-axis/y-axis denote the null/alternative hypotheses.

ing the neutrino signal from a future galactic CCSN. Our findings demonstrate a promising prospect: with a sufficiently large number of observed events (exceeding a few hundred), there exists a high probability of distinguishing between different FC scenarios based on the neutrino signals emitted by the next galactic CCSN.

In our analysis, we examine two distinct neutrino energy spectra designed to characterize the neutrino spectra throughout the SN accretion phase. One spectrum exhibits more pronounced variations among neutrino species, while the other displays comparatively mi-

nor fluctuations. Our findings illustrate that while distinguishing among the FC scenarios may be more discernible in the former spectrum, there remains a considerable probability of distinguishing between different FC scenarios even in cases where spectral differences are less pronounced.

In addition, in our calculations, we incorporate two distinct neutrino detection channels: IBD and ES. While the ES channel exhibits sensitivity to all neutrino species and possesses the potential to distinguish among different neutrino flavors, our findings illustrate that the crucial factor here lies in the events number. Surprisingly, our results indicate that incorporating the ES channel does not significantly enhance our analysis due to its relatively lower number of events.

In realistic scenarios it is crucial to consider two important factors. The first is that neutrinos may encounter FC scenarios with MSW effect on top. This means they could undergo flavor conversions deep within the SN core while also experiencing the MSW effect at larger radii. Moreover, the spectral parameters of neutrinos might remain unknown at the time of detection, which necessitates an optimization to finding the spectral parameters. Our findings demonstrate that both these effects unfavorably impact our ability to distinguish among different FC scenarios and increase the minimum number of events required for efficient FC scenario differentiation.

In summary, our findings highlight the potential to differentiate various FC scenarios within the SN environment by analyzing a future SN neutrino signal. However, there remain crucial paths for further investigation. Primarily, our calculations excluded any information regarding the SN models. One can, in principle, link various FC scenarios to SN models derived from CCSN simulations. This connection has been explored to some extent in the studies detailed in Refs. [15–17], though only focusing on the MSW effect. The incorporation of SN models has the

potential to improve the ability to differentiate between FC scenarios in calculations where spectral parameters are unknown. However, it is crucial to note that introducing the complexity of various SN models might simultaneously hinder the distinguishability of different FC scenarios by introducing a potential degeneracy. Additionally, our FC scenarios presumed perfect conversions, which may not hold true in reality. For example, the MSW effect might not achieve complete adiabaticity, resulting in final flux values deviating from those of an ideal adiabatic MSW scenario. Similar uncertainties could exist in other FC scenarios, where actual equipartition might only be partial, differing from our assumed perfect conditions. Assessing the distinguishability of various FC scenarios under partial conversions would be a valuable exploration. Furthermore, our focus was solely on the IBD and ES detection channels. While our results suggest that incorporating the ES channel does not significantly impact our analysis, this might differ for other available neutrino detection channels. Considering the imperative

need to comprehend neutrino FC mechanisms within the SN environment, addressing these crucial aspects significantly enhance our ability to extract insights from the neutrino signal of a future galactic CCSN.

ACKNOWLEDGMENTS

S.A. is deeply grateful to Georg Raffelt for insightful conversations. S.A. was supported by the German Research Foundation (DFG) through the Collaborative Research Centre “Neutrinos and Dark Matter in Astro- and Particle Physics (NDM),” Grant SFB-1258, and under Germany’s Excellence Strategy through the Cluster of Excellence ORIGINS EXC-2094-390783311. We would also like to acknowledge the use of the following softwares: SCIKIT-LEARN [70], KERAS [71], MATPLOTLIB [72], NUMPY [73], SCIPY [74], and IPYTHON [75].

-
- [1] S. Horiuchi, J. P. Kneller, What can be learned from a future supernova neutrino detection?, *J. Phys. G* 45 (4) (2018) 043002. [arXiv:1709.01515](#), [doi:10.1088/1361-6471/aaa90a](#).
 - [2] G. G. Raffelt, Supernova neutrino observations: What can we learn?, *Nucl. Phys. B Proc. Suppl.* 221 (2011) 218–229. [arXiv:astro-ph/0701677](#), [doi:10.1016/j.nuclphysbps.2011.09.006](#).
 - [3] H. T. Janka, Neutrino-driven Explosions (2 2017). [arXiv:1702.08825](#), [doi:10.1007/978-3-319-21846-5_109](#).
 - [4] M. C. Volpe, Neutrinos from dense: flavor mechanisms, theoretical approaches, observations, new directions, *arXiv e-prints* (2023). [arXiv:2301.11814](#).
 - [5] T. J. Loredo, D. Q. Lamb, Bayesian analysis of neutrinos observed from supernova SN-1987A, *Phys. Rev. D* 65 (2002) 063002. [arXiv:astro-ph/0107260](#), [doi:10.1103/PhysRevD.65.063002](#).
 - [6] G. Pagliaroli, F. Vissani, M. L. Costantini, A. Ianni, Improved analysis of SN1987A antineutrino events, *Astropart. Phys.* 31 (2009) 163–176. [arXiv:0810.0466](#), [doi:10.1016/j.astropartphys.2008.12.010](#).
 - [7] A. Harada, Y. Suwa, M. Harada, Y. Koshio, M. Mori, F. Nakanishi, K. Nakazato, K. Sumiyoshi, R. A. Wendell, Observing Supernova Neutrino Light Curves with Super-Kamiokande. IV. Development of SPECIAL BLEND: A New Public Analysis Code for Supernova Neutrinos, *Astrophys. J.* 954 (1) (2023) 52. [arXiv:2304.05437](#), [doi:10.3847/1538-4357/ace52e](#).
 - [8] A. Gallo Rosso, S. Abbar, F. Vissani, M. C. Volpe, Late time supernova neutrino signal and proto-neutron star radius, *JCAP* 12 (2018) 006. [arXiv:1809.09074](#), [doi:10.1088/1475-7516/2018/12/006](#).
 - [9] A. Gallo Rosso, F. Vissani, M. C. Volpe, What can we learn on supernova neutrino spectra with water Cherenkov detectors?, *JCAP* 04 (2018) 040. [arXiv:1712.05584](#), [doi:10.1088/1475-7516/2018/04/040](#).
 - [10] Y. Suwa, A. Harada, M. Harada, Y. Koshio, M. Mori, F. Nakanishi, K. Nakazato, K. Sumiyoshi, R. A. Wendell, Observing Supernova Neutrino Light Curves with Super-Kamiokande. III. Extraction of Mass and Radius of Neutron Stars from Synthetic Data (4 2022). [arXiv:2204.08363](#), [doi:10.3847/1538-4357/ac795e](#).
 - [11] A. Gallo Rosso, F. Vissani, M. C. Volpe, Measuring the neutron star compactness and binding energy with supernova neutrinos, *JCAP* 11 (2017) 036. [arXiv:1708.00760](#), [doi:10.1088/1475-7516/2017/11/036](#).
 - [12] E. W. Kolb, M. S. Turner, Supernova SN 1987a and the Secret Interactions of Neutrinos, *Phys. Rev. D* 36 (1987) 2895. [doi:10.1103/PhysRevD.36.2895](#).
 - [13] S. Shalgar, I. Tamborra, M. Bustamante, Core-collapse supernovae stymie secret neutrino interactions, *Phys. Rev. D* 103 (12) (2021) 123008. [arXiv:1912.09115](#), [doi:10.1103/PhysRevD.103.123008](#).
 - [14] A. de Gouvêa, I. Martinez-Soler, Y. F. Perez-Gonzalez, M. Sen, Diffuse supernova neutrino background as a probe of late-time neutrino mass generation, *Phys. Rev. D* 106 (10) (2022) 103026. [arXiv:2205.01102](#), [doi:10.1103/PhysRevD.106.103026](#).
 - [15] K. Abe, et al., Supernova Model Discrimination with Hyper-Kamiokande, *Astrophys. J.* 916 (1) (2021) 15. [arXiv:2101.05269](#), [doi:10.3847/1538-4357/abf7c4](#).
 - [16] J. Olsen, Y.-Z. Qian, Prospects for distinguishing supernova models using a future neutrino signal, *Phys. Rev. D* 105 (8) (2022) 083017. [arXiv:2202.09975](#), [doi:10.1103/PhysRevD.105.083017](#).
 - [17] M. M. Saez, E. Rrapaj, A. Harada, S. Nagataki, Y.-Z. Qian, Correlations and Distinguishability Challenges in Supernova Models: Insights from Future Neutrino Detectors (1 2024). [arXiv:2401.02531](#).
 - [18] J. T. Pantaleone, Neutrino oscillations at high densities, *Phys. Lett. B* 287 (1992) 128–132. [doi:10.1016/0370-2693\(92\)91887-F](#).
 - [19] G. Sigl, G. Raffelt, General kinetic description of relativistic mixed neutrinos, *Nuclear Physics B* 406 (1)

- (1993) 423–451. [doi:10.1016/0550-3213\(93\)90175-0](#).
- [20] S. Pastor, G. Raffelt, Flavor oscillations in the supernova hot bubble region: Nonlinear effects of neutrino background, *Phys. Rev. Lett.* 89 (2002) 191101. [arXiv:astro-ph/0207281](#), [doi:10.1103/PhysRevLett.89.191101](#).
- [21] H. Duan, G. M. Fuller, J. Carlson, Y.-Z. Qian, Simulation of Coherent Non-Linear Neutrino Flavor Transformation in the Supernova Environment. 1. Correlated Neutrino Trajectories, *Phys. Rev. D* 74 (2006) 105014. [arXiv:astro-ph/0606616](#), [doi:10.1103/PhysRevD.74.105014](#).
- [22] H. Duan, G. M. Fuller, J. Carlson, Y.-Z. Qian, Coherent Development of Neutrino Flavor in the Supernova Environment, *Phys. Rev. Lett.* 97 (2006) 241101. [arXiv:astro-ph/0608050](#), [doi:10.1103/PhysRevLett.97.241101](#).
- [23] H. Duan, G. M. Fuller, Y.-Z. Qian, Collective Neutrino Oscillations, *Ann. Rev. Nucl. Part. Sci.* 60 (2010) 569–594. [arXiv:1001.2799](#), [doi:10.1146/annurev.nucl.012809.104524](#).
- [24] A. Mirizzi, I. Tamborra, H.-T. Janka, N. Saviano, K. Scholberg, R. Bollig, L. Hudepohl, S. Chakraborty, Supernova neutrinos: Production, oscillations and detection, *Riv. Nuovo Cim.* 39 (1-2) (2016) 1–112. [arXiv:1508.00785](#), [doi:10.1393/ncr/i2016-10120-8](#).
- [25] B. Dasgupta, A. Dighe, G. G. Raffelt, A. Y. Smirnov, Multiple Spectral Splits of Supernova Neutrinos, *Phys. Rev. Lett.* 103 (2009) 051105. [arXiv:0904.3542](#), [doi:10.1103/PhysRevLett.103.051105](#).
- [26] S. Galais, C. Volpe, The neutrino spectral split in core-collapse supernovae: a magnetic resonance phenomenon, *Phys. Rev. D* 84 (2011) 085005. [arXiv:1103.5302](#), [doi:10.1103/PhysRevD.84.085005](#).
- [27] B. Dasgupta, Collective Neutrino Flavor Instability Requires a Crossing, *Phys. Rev. Lett.* 128 (8) (2022) 081102. [arXiv:2110.00192](#), [doi:10.1103/PhysRevLett.128.081102](#).
- [28] R. F. Sawyer, Speed-up of neutrino transformations in a supernova environment, *Phys. Rev. D* 72 (4) (2005) 045003. [arXiv:hep-ph/0503013](#), [doi:10.1103/PhysRevD.72.045003](#).
- [29] R. F. Sawyer, Neutrino Cloud Instabilities Just above the Neutrino Sphere of a Supernova, *Phys. Rev. Lett.* 116 (8) (2016) 081101. [arXiv:arXiv:1509.03323](#), [doi:10.1103/PhysRevLett.116.081101](#).
- [30] T. Morinaga, Fast neutrino flavor instability and neutrino flavor lepton number crossings, *Phys. Rev. D* 105 (10) (2022) L101301. [arXiv:2103.15267](#), [doi:10.1103/PhysRevD.105.L101301](#).
- [31] S. Abbar, Collective Oscillations of Majorana Neutrinos in Strong Magnetic Fields and Self-induced Flavor Equilibrium, *Phys. Rev. D* 101 (10) (2020) 103032. [arXiv:2001.04876](#), [doi:10.1103/PhysRevD.101.103032](#).
- [32] H. Sasaki, T. Takiwaki, Neutrino-antineutrino oscillations induced by strong magnetic fields in dense matter, *Phys. Rev. D* 104 (2) (2021) 023018. [arXiv:2106.02181](#), [doi:10.1103/PhysRevD.104.023018](#).
- [33] O. G. Kharlanov, P. I. Shustov, Effects of nonstandard neutrino self-interactions and magnetic moment on collective Majorana neutrino oscillations, *Phys. Rev. D* 103 (9) (2021) 095004. [arXiv:2010.05329](#), [doi:10.1103/PhysRevD.103.095004](#).
- [34] S. Abbar, Nonstandard neutrino self-interactions can cause neutrino flavor equipartition inside the supernova core, *Phys. Rev. D* 107 (10) (2023) 103002. [arXiv:2208.06023](#), [doi:10.1103/PhysRevD.107.103002](#).
- [35] C. J. Stapleford, D. J. Väänänen, J. P. Kneller, G. C. McLaughlin, B. T. Shapiro, Nonstandard Neutrino Interactions in Supernovae, *Phys. Rev. D* 94 (9) (2016) 093007. [arXiv:1605.04903](#), [doi:10.1103/PhysRevD.94.093007](#).
- [36] P. D. Serpico, S. Chakraborty, T. Fischer, L. Hudepohl, H.-T. Janka, A. Mirizzi, Probing the neutrino mass hierarchy with the rise time of a supernova burst, *Phys. Rev. D* 85 (2012) 085031. [arXiv:1111.4483](#), [doi:10.1103/PhysRevD.85.085031](#).
- [37] T. Fischer, S. C. Whitehouse, A. Mezzacappa, F. K. Thielemann, M. Liebendorfer, Protoneutron star evolution and the neutrino driven wind in general relativistic neutrino radiation hydrodynamics simulations, *Astrophys. J.* 517 (2010) A80. [arXiv:0908.1871](#), [doi:10.1051/0004-6361/200913106](#).
- [38] A. S. Dighe, A. Y. Smirnov, Identifying the neutrino mass spectrum from the neutrino burst from a supernova, *Phys. Rev. D* 62 (2000) 033007. [arXiv:hep-ph/9907423](#), [doi:10.1103/PhysRevD.62.033007](#).
- [39] J. D. Martin, J. Carlson, H. Duan, Spectral swaps in a two-dimensional neutrino ring model, *Phys. Rev. D* 101 (2) (2020) 023007. [arXiv:1911.09772](#), [doi:10.1103/PhysRevD.101.023007](#).
- [40] G. G. Raffelt, G. Sigl, Self-induced decoherence in dense neutrino gases, *Phys. Rev. D* 75 (2007) 083002. [arXiv:hep-ph/0701182](#), [doi:10.1103/PhysRevD.75.083002](#).
- [41] J. Ehring, S. Abbar, H.-T. Janka, G. Raffelt, I. Tamborra, Fast Neutrino Flavor Conversions Can Help and Hinder Neutrino-Driven Explosions, *Phys. Rev. Lett.* 131 (6) (2023) 061401. [arXiv:2305.11207](#), [doi:10.1103/PhysRevLett.131.061401](#).
- [42] J. Ehring, S. Abbar, H.-T. Janka, G. Raffelt, I. Tamborra, Fast neutrino flavor conversion in core-collapse supernovae: A parametric study in 1D models, *Phys. Rev. D* 107 (10) (2023) 103034. [arXiv:2301.11938](#), [doi:10.1103/PhysRevD.107.103034](#).
- [43] R. F. Sawyer, Speed-up of neutrino transformations in a supernova environment, *Phys. Rev. D* 72 (2005) 045003. [arXiv:hep-ph/0503013](#), [doi:10.1103/PhysRevD.72.045003](#).
- [44] R. F. Sawyer, Neutrino cloud instabilities just above the neutrino sphere of a supernova, *Phys. Rev. Lett.* 116 (8) (2016) 081101. [arXiv:1509.03323](#), [doi:10.1103/PhysRevLett.116.081101](#).
- [45] S. Chakraborty, R. S. Hansen, I. Izaguirre, G. Raffelt, Self-induced neutrino flavor conversion without flavor mixing, *JCAP* 03 (2016) 042. [arXiv:1602.00698](#), [doi:10.1088/1475-7516/2016/03/042](#).
- [46] S. Bhattacharyya, B. Dasgupta, Late-time behavior of fast neutrino oscillations, *Phys. Rev. D* 102 (6) (2020) 063018. [arXiv:2005.00459](#), [doi:10.1103/PhysRevD.102.063018](#).
- [47] S. Bhattacharyya, B. Dasgupta, Fast Flavor Depolarization of Supernova Neutrinos, *Phys. Rev. Lett.* 126 (6) (2021) 061302. [arXiv:2009.03337](#), [doi:10.1103/PhysRevLett.126.061302](#).
- [48] M.-R. Wu, M. George, C.-Y. Lin, Z. Xiong, Collective fast neutrino flavor conversions in a 1D box: Initial conditions and long-term evolution, *Phys. Rev. D* 104 (10) (2021) 103003. [arXiv:2108.09886](#), [doi:10.1103/PhysRevD.104.103003](#).

- [49] S. Richers, D. E. Willcox, N. M. Ford, A. Myers, Particle-in-cell Simulation of the Neutrino Fast Flavor Instability, *Phys. Rev. D* 103 (8) (2021) 083013. [arXiv:2101.02745](#), [doi:10.1103/PhysRevD.103.083013](#).
- [50] M. Zaizen, T. Morinaga, Nonlinear evolution of fast neutrino flavor conversion in the preshock region of core-collapse supernovae, *Phys. Rev. D* 104 (8) (2021) 083035. [arXiv:2104.10532](#), [doi:10.1103/PhysRevD.104.083035](#).
- [51] S. Richers, D. Willcox, N. Ford, Neutrino fast flavor instability in three dimensions, *Phys. Rev. D* 104 (10) (2021) 103023. [arXiv:2109.08631](#), [doi:10.1103/PhysRevD.104.103023](#).
- [52] S. Bhattacharyya, B. Dasgupta, Elaborating the ultimate fate of fast collective neutrino flavor oscillations, *Phys. Rev. D* 106 (10) (2022) 103039. [arXiv:2205.05129](#), [doi:10.1103/PhysRevD.106.103039](#).
- [53] E. Grohs, S. Richers, S. M. Couch, F. Foucart, J. P. Kneller, G. C. McLaughlin, Neutrino fast flavor instability in three dimensions for a neutron star merger, *Phys. Lett. B* 846 (2023) 138210. [arXiv:2207.02214](#), [doi:10.1016/j.physletb.2023.138210](#).
- [54] S. Abbar, F. Capozzi, Suppression of fast neutrino flavor conversions occurring at large distances in core-collapse supernovae, *JCAP* 03 (03) (2022) 051. [arXiv:2111.14880](#), [doi:10.1088/1475-7516/2022/03/051](#).
- [55] S. Richers, H. Duan, M.-R. Wu, S. Bhattacharyya, M. Zaizen, M. George, C.-Y. Lin, Z. Xiong, Code comparison for fast flavor instability simulations, *Phys. Rev. D* 106 (4) (2022) 043011. [arXiv:2205.06282](#), [doi:10.1103/PhysRevD.106.043011](#).
- [56] M. Zaizen, H. Nagakura, Simple method for determining asymptotic states of fast neutrino-flavor conversion, *Phys. Rev. D* 107 (10) (2023) 103022. [arXiv:2211.09343](#), [doi:10.1103/PhysRevD.107.103022](#).
- [57] Z. Xiong, M.-R. Wu, S. Abbar, S. Bhattacharyya, M. George, C.-Y. Lin, Evaluating approximate asymptotic distributions for fast neutrino flavor conversions in a periodic 1D box, *Phys. Rev. D* 108 (6) (2023) 063003. [arXiv:2307.11129](#), [doi:10.1103/PhysRevD.108.063003](#).
- [58] J. Cernohorsky, S. A. Bludman, Maximum entropy distribution and closure for Bose-Einstein and Fermi-Dirac radiation transport (3 1994).
- [59] Z. Bialynicka-Birula, Do Neutrinos Interact between Themselves?, *Nuovo Cim.* 33 (1964) 1484–1487. [doi:10.1007/BF02749481](#).
- [60] D. Y. Bardin, S. M. Bilenky, B. Pontecorvo, On the ν - ν interaction, *Phys. Lett. B* 32 (1970) 121–124. [doi:10.1016/0370-2693\(70\)90602-7](#).
- [61] C. Giunti, A. Studenikin, Neutrino electromagnetic properties, *Phys. Atom. Nucl.* 72 (2009) 2089–2125. [arXiv:0812.3646](#), [doi:10.1134/S1063778809120126](#).
- [62] C. Brogini, C. Giunti, A. Studenikin, Electromagnetic Properties of Neutrinos, *Adv. High Energy Phys.* 2012 (2012) 459526. [arXiv:1207.3980](#), [doi:10.1155/2012/459526](#).
- [63] A. Studenikin, Status and perspectives of neutrino magnetic moments, *J. Phys. Conf. Ser.* 718 (6) (2016) 062076. [arXiv:1603.00337](#), [doi:10.1088/1742-6596/718/6/062076](#).
- [64] P. Mösta, C. D. Ott, D. Radice, L. F. Roberts, E. Schnetter, R. Haas, A large scale dynamo and magnetoturbulence in rapidly rotating core-collapse supernovae, *Nature* 528 (2015) 376. [arXiv:1512.00838](#), [doi:10.1038/nature15755](#).
- [65] K. Abe, et al., Hyper-Kamiokande Design Report (5 2018). [arXiv:1805.04163](#).
- [66] Y. Fukuda, et al., The Super-Kamiokande detector, *Nucl. Instrum. Meth. A* 501 (2003) 418–462. [doi:10.1016/S0168-9002\(03\)00425-X](#).
- [67] A. Strumia, F. Vissani, Precise quasielastic neutrino/nucleon cross-section, *Phys. Lett. B* 564 (2003) 42–54. [arXiv:astro-ph/0302055](#), [doi:10.1016/S0370-2693\(03\)00616-6](#).
- [68] J. A. Formaggio, G. P. Zeller, From eV to EeV: Neutrino Cross Sections Across Energy Scales, *Rev. Mod. Phys.* 84 (2012) 1307–1341. [arXiv:1305.7513](#), [doi:10.1103/RevModPhys.84.1307](#).
- [69] O. Tomalak, R. J. Hill, Theory of elastic neutrino-electron scattering, *Phys. Rev. D* 101 (3) (2020) 033006. [arXiv:1907.03379](#), [doi:10.1103/PhysRevD.101.033006](#).
- [70] F. Pedregosa, G. Varoquaux, A. Gramfort, V. Michel, B. Thirion, O. Grisel, M. Blondel, P. Prettenhofer, R. Weiss, V. Dubourg, et al., Scikit-learn: Machine learning in python, *Journal of machine learning research* 12 (Oct) (2011) 2825–2830.
- [71] F. Chollet, et al., Keras, <https://keras.io> (2015).
- [72] J. D. Hunter, Matplotlib: A 2d graphics environment, *Computing in Science & Engineering* 9 (3) (2007) 90–95. [doi:10.1109/MCSE.2007.55](#).
- [73] S. van der Walt, S. C. Colbert, G. Varoquaux, The numpy array: A structure for efficient numerical computation, *Computing in Science & Engineering* 13 (2) (2011) 22–30. [doi:10.1109/MCSE.2011.37](#).
- [74] P. Virtanen, R. Gommers, T. E. Oliphant, M. Haberland, T. Reddy, D. Cournapeau, E. Burovski, P. Peterson, W. Weckesser, J. Bright, S. J. van der Walt, M. Brett, J. Wilson, K. J. Millman, N. Mayorov, A. R. J. Nelson, E. Jones, R. Kern, E. Larson, C. J. Carey, Í. Polat, Y. Feng, E. W. Moore, J. VanderPlas, D. Laxalde, J. Perktold, R. Cimrman, I. Henriksen, E. A. Quintero, C. R. Harris, A. M. Archibald, A. H. Ribeiro, F. Pedregosa, P. van Mulbregt, SciPy 1.0 Contributors, SciPy 1.0: Fundamental Algorithms for Scientific Computing in Python, *Nature Methods* 17 (2020) 261–272. [doi:10.1038/s41592-019-0686-2](#).
- [75] F. Pérez, B. E. Granger, IPython: a system for interactive scientific computing, *Computing in Science and Engineering* 9 (3) (2007) 21–29. [doi:10.1109/MCSE.2007.53](#). URL <https://ipython.org>